Nb-depleted, continental rift-related Akaz metavolcanic rocks (West Kunlun): implication for the rifting of the Tarim Craton from Gondwana

CHAO YUAN[1,2], MIN SUN[2], JINGSUI YANG[3], HUI ZHOU[4] & MEI-FU ZHOU[2]

[1]*Guangzhou Institute of Geochemistry, Chinese Academy of Sciences, Guangzhou 510640, China*

[2]*Department of Earth Sciences, The University of Hong Kong, Pokfulam Road, Hong Kong, China (e-mail: minsun@hkucc.hku.hk)*

[3]*Institute of Geology, Chinese Academy of Geological Sciences, 26 Baiwanzhuang Road, Beijing 100073*

[4]*Department of Geology, Peking University, Beijing 100871, China*

Abstract: The Akaz metavolcanic rocks of the West Kunlun Mountains possess low to intermediate SiO_2 (42.3–64.7 wt%) and MgO (2.69–7.54 wt%) and high TiO_2 (0.94–3.05 wt%) and $Fe_2O_3^T$ (7.64–18.47 wt%), indicating a basaltic to andesitic protolith. These rocks have high contents of Zr (89.6–470 ppm), Nb (10.0–40.3 ppm), Y (19.7–52.7 ppm), Th (0.86–15.96 ppm) and total REE (67.7–407 ppm), and are characterized by relatively high Ti/Y (183–649), Th/Yb (0.5–3.9), and low Hf/Ta (3.0–8.6) ratios. They are LREE-enriched (La/Yb = 5.4–20) and most have small negative Nb anomalies (Nb/Nb* = 0.20–1.16). These characteristics are transitional between within-plate and subduction-related basalts. The relatively high Gd/Yb ratios (1.4–2.9) distinguish these rocks from island-arc tholeiites and the high Zr/Y (3–12), Ta/Yb (0.3–0.7) and low Zr/Nb (<12) ratios strongly support a continental affinity. The protoliths for the Akaz metavolcanic rocks are interpreted to be continental rift basalts formed during rifting of the Tarim Craton from Gondwana. Stratigraphic and palaeontological data indicate that the rifting occurred in Sinian to Cambrian times, roughly contemporaneously with rifting in the East Kunlun and North Qilian orogenic belts farther to the east.

Understanding the tectonic evolution of the Western Kunlun mountain range is important for unravelling the early history of the Tibetan Plateau. A previously proposed collisional model envisaged the West Kunlun as a tectonic collage composed of a continental block (North Kunlun Block) and an accreted arc terrane (South Kunlun Block) (Yao & Hsü 1994; Hsü *et al.* 1995; Sengör & Natal'in 1996; Li *et al.* 1999; Xiao *et al.* 2002). However, an alternative model considers both the North and South Kunlun blocks to be parts of the Tarim Craton (Pan *et al.* 1994; Ding *et al.* 1996; Mattern *et al.* 1996; Mattern & Schneider 2000). The Tarim Craton itself, as a major block of the Chinese continent (Fig. 1), was originally part of Gondwana. The Tarim Craton was rifted from Gondwana by the opening of the Tethyan ocean (*sensu lato*) (Li *et al.* 1991; Li *et al.* 1996; Metcalfe 1996; Zhao *et al.* 1996; Li 1998; Stampfli & Borel 2002). The Akaz meta-volcanic sequence in the West Kunlun crops out along the south margin of the North Kunlun Block, and may provide critical constraints on the above tectonic models. The sequence is considered to be the result of Neoproterozoic continental rifting (Pan *et al.* 1994), or to be part of a seamount accreted during subduction of the Tethyan ocean basin (Xiao *et al.* 2002). These different interpretations stem from the lack of a comprehensive geochemical study of the volcanic rocks. In this paper, we present new systematic geochemical data for the Akaz metavolcanic rocks, and use these data to constrain their petrogenesis and to shed light on the tectonic evolution of the West Kunlun.

Geological setting

The Tibetan Plateau was formed by the successive accretion of several microcontinental and arc blocks from Gondwana to the Laurasian continent (Chang *et al.* 1986; Molnar *et al.* 1987;

From: MALPAS, J., FLETCHER, C. J. N., ALI, J. R. & AITCHISON, J. C. (eds) 2004. *Aspects of the Tectonic Evolution of China*. Geological Society, London, Special Publications, **226**, 131–143.
0305-8719/04/$15

Dewey *et al.* 1988; Yin & Harrison 2000) (Fig. 1). These accreted blocks are separated by several suture zones that young progressively to the south. The Kunlun Mountains in the northernmost part of the Plateau are divided by the Altyn Tagh Fault into eastern and western segments (Fig. 1). The West Kunlun consists of the North Kunlun and South Kunlun Blocks, separated by the early Paleozoic Kudi–Subashi suture (Pan *et al.* 1994; Matte *et al.* 1996; Yang *et al.* 1996) (Fig. 1). The North Kunlun Block is in fault contact with the Tarim Craton in the north, whereas the South Kunlun Block is bounded by the strike-slip Karakash Fault to the south (Matte *et al.* 1996), which is coincident with one of the sutures of the Palaeo-Tethys (Pan *et al.* 1994; Mattern *et al.* 1996) (Fig. 1).

The basement of the North Kunlun Block consists of the Precambrian Ailiankate Complex, made up of metaclastic and carbonate rocks with subordinate metavolcanic rocks (Wen *et al.* 2000) (Figs 2 and 3). These rocks were intruded by 2.2 Ga granitic plutons (Xu *et al.* 1994) suggesting that the Precambrian basement of the North Kunlun Block and the Tarim Craton are the same (Pan *et al.* 1994; Hsü *et al.* 1995; Ding *et al.* 1996; Matte *et al.* 1996; Mattern & Schneider 2000; Yuan *et al.* 2002, 2003; Xiao *et al.* 2002).

The Sailajaz Tagh Group, a metavolcanic sequence with some interlayered metasedimentary rocks, unconformably overlies the Ailiankate Complex (Fig. 2). The metavolcanic sequence occurs in the lower part of the Sailajaz Tagh Group, and is referred to as the Akaz greenschist in the literature (Deng 1989; Pan *et al.* 1994; Wen *et al.* 2000) (Fig. 3). These metavolcanic rocks include basalt, spilite, quartz-keratophyre, felsite-porphyry, potash keratophyre and rhyolite, intercalated with silicic and mafic tuff. Thin

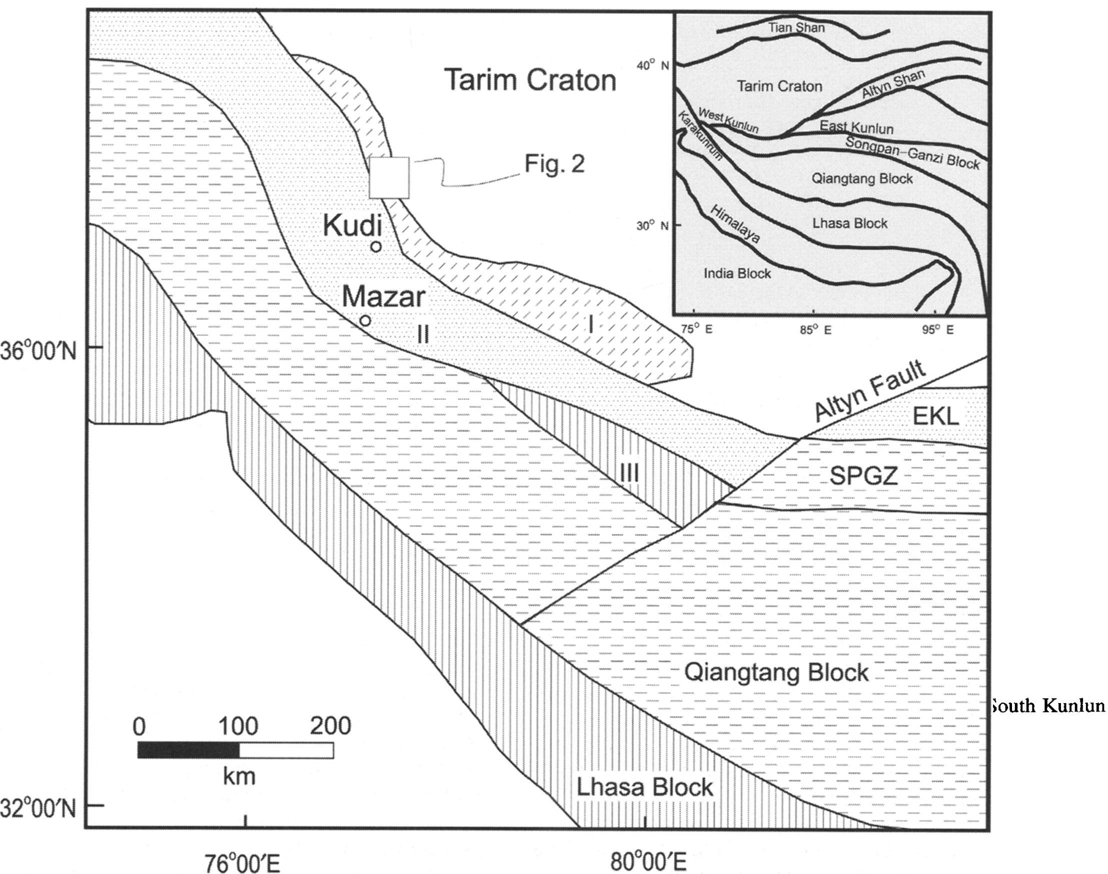

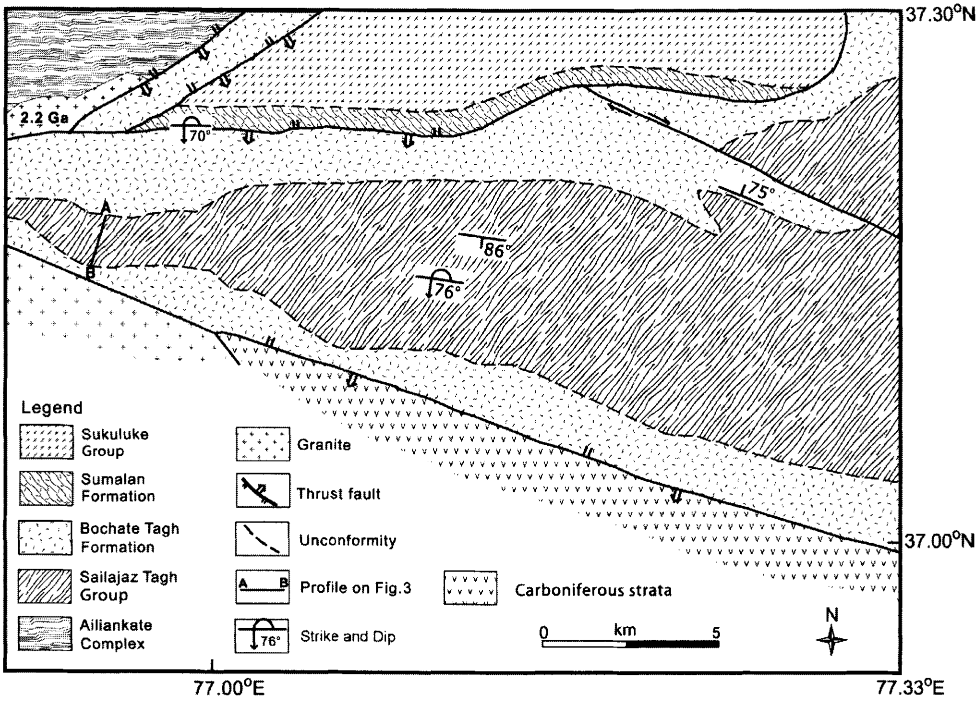

Fig. 2. Geological map of the Akaz pass area, western Kunlun Mountains (modified from XGIT-II 1985).

layers or lenses of metamorphosed sandstone, siltstone and limestone are intercalated with the metavolcanic rocks (XGIT-II 1985) and the entire sequence is conformably overlain by dolomite, marble, phyllite, sandstone and schist. The relative abundance of metavolcanic rocks in the Sailajaz Group increases from east to west, where they become dominant.

Samples for this study were collected in the Akaz Pass, where the Xinjiang–Tibet road transects the western part of the Sailajaz Tagh Group and exposes the entire metavolcanic sequence (Figs 2 and 3). The metavolcanic rocks in this area are dominantly basalt and basaltic andesite flows with sparse tuff (Deng 1989). Six layers of metavolcanic rocks, from 20 to more than 100 m thick, crop out south of the Akaz Pass. The bottom layer is massive and relatively fresh, whereas the other layers are variably fractured, altered and decomposed due to neotectonic activity and weathering. Twenty samples were collected at regular intervals across the bottom layer at milestone 124.6 (Fig. 2).

Isotope geochronological data are not currently available for the Sailajaz Tagh Group. The unit has been tentatively placed in the Sinian (Late Neoproterozoic) or Cambrian, because it contains stromatolites and crinoid fossils and is unconformably overlain by Devonian to Triassic strata (Pan *et al.* 1994; Xiao *et al.* 2002). To the east, Cambrian rift-related volcanic rocks have been recognized in East Kunlun (Fig. 1) (Pan *et al.* 1996). Even farther east, in the North Qilian Mountains, single-grain zircon dating and whole-rock Sm–Nd dating of rift-related volcanic rocks yielded ages of 738–604 Ma and 522 to 593 Ma, respectively (Xia *et al.* 1996; Mao *et al.* 1998; Xia *et al.* 1999). These ages are thought to be roughly consistent with that of the Akaz metavolcanic rocks in the West Kunlun.

Petrography

The Akaz metavolcanic samples consist of chlorite, epidote, albite, quartz, calcite, and magnetite with, or without, biotite. Some samples (GS-13, 14, 18, 19 and 21) contain zoisite instead of epidote. Three samples (GS-13, 15 and 19) have relatively few mafic minerals, but more quartz and feldspar, and contain biotite that does not occur in other samples. The chlorite, epidote and albite are anhedral to subhedral, and most albite crystals do not show polysynthetic twinning. Muscovite was identified in one sample (GS-13).

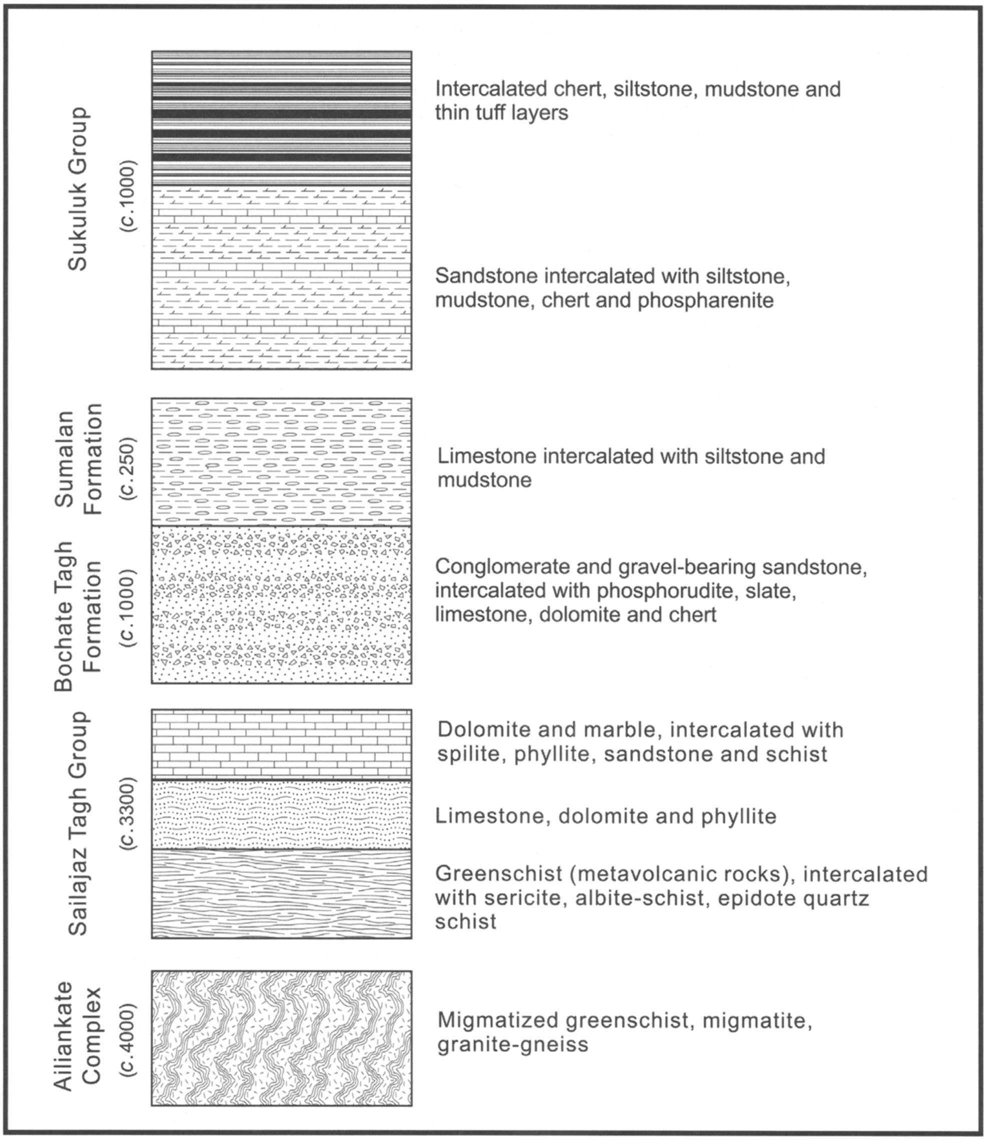

Fig. 3. Stratigraphic column of the North Kunlun Block, West Kunlun Mountains (XGIT-II, 1985 and Wen *et al.* 2000). Estimated thickness of units in metres given in brackets.

The Akaz metavolcanic samples are strongly deformed, and the original textures and structures are mostly obliterated. These metavolcanic rocks exhibit schistosity, comprised of green bands of chlorite and epidote and light-coloured bands of albite and quartz. The metamorphic mineral compositions and textures of the rocks indicate low-temperature and moderate-pressure greenschist-facies metamorphism (Williams *et al.* 1989).

Analytical methods

Whole-rock samples were crushed using a jaw crusher, and the resulting chips were cleaned three times with de-ionized water in an ultrasonic vessel (15 minutes each time), dried and then ground into powder using an agate mill. Samples were dissolved with mixed acid (HF + HNO_3) in Teflon screw-capped vials to ensure complete digestion. Major oxides were measured on a Varian

VISTA-PRO ICP–AES in the Guangzhou Institute of Geochemistry, Chinese Academy of Sciences, whereas trace elements were analysed on a Perkin Elmer Elan 6000 ICP–MS, installed in the same institute. Chinese (GSR1-5) and international rock standards (W-2, MRG-1, G-1, SY-4 and GSP-1) were used as either reference materials or external standards to monitor the analytical accuracy. Samples were separately dissolved using the NaOH sinter method and measured for SiO_2 content with the ICP–AES. The precision for major oxides is within 0.5–1% RSD (relative standard deviation), whereas those for trace elements are better than 5% (for Rb, Sr, Cs, Ba, Y, Zr, Nb, Ta, U, Th, and Hf or 3% RSD rare-earth elements (REEs). The results are presented in Table 1.

Analytical results

The Akaz metavolcanic rocks vary widely in SiO_2 contents (42–64 wt%), but the majority fall between 45 and 55 wt%. The Al_2O_3 (12.18–16.91 wt%) and $Fe_2O_3^T$ (*c*.18.47 wt%) contents fall within the range of MORB compositions, but they have relatively low MgO (2.69–7.54 wt%) and P_2O_5 (0.08–0.36 wt%), and relatively high TiO_2 (0.94–3.05 wt%) concentrations.

All the samples in this study exhibit LREE-enriched patterns (La/Yb = 5.4–20), with various Eu anomalies (Eu/Eu* = 0.74–1.4) and slightly negative Ce (Ce/Ce* = 0.87–0.97) anomalies (Table 1; Fig. 4). Most samples have LILE and HFSE concentrations higher than those of E-MORB (Sun & McDonough 1989), but very similar to those of the Deccan continental flood basalts (e.g. Wilson 1989) (Table 1; Fig. 5). Their high La–Nb (0.92–2.49) and Th–Nb (0.09–1.29) ratios indicate considerable HFSE depletion relative to LILE (Table 1). Most samples show various degree of Nb depletion (Nb/Nb* = 0.20–0.65) in spider diagrams (Fig. 5) and the most Nb-depleted sample GS-19 (Nb/Nb* = 0.20) has the highest SiO_2 (64.7 wt%) and the lowest P_2O_5 (0.08 wt%) and TiO_2 (0.94 wt%) contents. Two samples (GS-7 and GS-18), with the lowest contents of LILE and HFSE have slightly positive Nb anomalies (Nb/Nb* *c*.1.16) (Fig. 5, Table 1).

Discussion

Nature of the Akaz metavolcanic rocks

Most Akaz metavolcanic samples are mafic in composition, although three samples are intermediate (SiO_2 = 54.2–55.1 wt%) and one sample (GS-19) is relatively silicic, with a SiO_2 content of 64.7 wt%. The relatively high TiO_2, $Fe_2O_3^T$ and MgO contents, although variable, are consistent with their mafic compositions. The rocks have variable CaO (2.05–9.96 wt%), K_2O (0.09–5.29 wt%), Na_2O (0.15–5.3 wt%) and LOI contents (1.94–8.53 wt%), reflecting the effects of hydrothermal alteration. Accordingly, only relatively immobile elements are reliable indicators of the protolith composition (Lightfoot 1993). Because Nb, Zr, Ti and Y are relatively insensitive to alteration, the Nb/Y v. Zr/TiO_2 diagram was used to classify the rocks. Most of the Akaz metavolcanic rocks plot in the field of subalkaline basalt, whereas the three samples with relatively high SiO_2 contents plot in the alkaline basalt (GS-16), trachyandesite (GS-13) and dacite (GS-19) fields (Fig. 6a), suggesting that the protoliths of the metavolcanic rocks are dominantly tholeiitic basalts. In the Mg# v. TiO_2 diagram, almost all the samples plot in the high-Ti tholeiite field (Fig. 6b). Their low Cr (77.3–238 ppm) and Ni (28.6–72.3) contents, suggest that all these samples were derived from an evolved magma.

Origin and tectonic setting of the Akaz metavolcanic rocks

Tholeiitic basalts can occur in a variety of tectonic settings, e.g. oceanic floor, oceanic plateau, oceanic island, seamount, island arc, back-arc basin and continental interior (Wilson 1989; Flower 1991; Floyd 1991; Saunders & Tarney 1991). The intermediate Nb/Y ratios and relatively high LILE (Th, U) and HFSE (Nb, Ta, Zr, Hf, Ti, Y) contents of the Akaz metavolcanic rocks suggest that the basaltic protolith might have been derived from an enriched mantle source.

The Akaz metavolcanic rocks have transitional geochemical signatures of between within-plate and subduction-related basalts. On one hand, the high contents of HFSE (e.g. Ti, Nb and Ta), relatively high Ti/Y (mostly >350) and low Hf/Ta (mostly <5) ratios make the rocks akin to within-plate basalts (Condie 1989). On the other hand, the negative Nb anomalies, relatively high Th/Nb (0.1–1.3), La/Nb (0.9–2.5) and Th/Yb (0.5–3.9) ratios show an arc-related signature for the metavolcanic rocks. Therefore, different tectonic discrimination diagrams give different results. For example, in the Zr-Zr/Y diagram, most of the Akaz samples plot in the within-plate basalt field (Pearce & Cann 1973) (Fig. 7a); whereas in the Ta/Yb v. Th/Yb

Table 1. *Representative chemical analyses of Akaz metavolcanics, West Kunlun*

Sample	GS-1	GS-2	GS-3	GS-4	GS-5	GS-6	GS-7	GS-8	GS-9	GS-10	GS-11	GS-12	GS-13	GS-14	GS-15	GS-16	GS-17	GS-18	GS-19	GS-21
SiO_2	48.59	45.69	54.23	50.43	44.96	43.51	46.37	46.00	46.23	49.92	47.30	49.84	55.13	50.16	47.10	54.33	42.33	46.00	64.70	45.15
TiO_2	1.95	3.05	2.28	2.06	2.67	2.37	2.13	2.18	2.18	2.13	2.19	1.98	1.83	2.25	2.12	1.98	2.98	1.96	0.94	2.37
Al_2O_3	12.63	16.91	14.38	13.06	16.85	14.92	13.04	14.00	14.03	13.21	13.91	12.63	14.77	12.18	13.75	13.72	13.6	14.05	12.53	14.85
$Fe_2O_3^T$	13.16	16.29	14.93	13.17	18.47	15.65	13.72	15.11	15.56	16.38	15.44	13.78	8.88	12.78	15.10	12.30	15.79	13.73	7.64	15.88
MnO	0.25	0.17	0.12	0.21	0.12	0.23	0.19	0.25	0.23	0.18	0.20	0.27	0.07	0.14	0.24	0.11	0.18	0.22	0.09	0.18
MgO	4.88	5.38	3.69	4.59	3.97	5.51	7.40	7.06	4.88	3.56	6.33	4.28	2.69	4.81	6.85	5.24	6.14	7.54	2.75	6.68
CaO	7.41	2.58	2.21	5.99	3.23	5.92	7.46	5.75	5.80	4.84	7.38	6.48	2.05	6.79	5.42	3.67	7.61	9.96	3.87	4.84
Na_2O	4.35	3.59	3.63	4.64	2.84	5.14	0.98	3.59	5.30	4.99	3.79	4.46	0.15	2.31	3.52	2.42	1.97	1.55	3.17	2.90
K_2O	0.09	2.42	2.00	0.14	3.44	0.34	2.21	0.11	0.22	0.60	0.29	0.33	5.29	3.47	0.12	3.12	3.59	1.53	2.27	1.66
P_2O_5	0.25	0.19	0.22	0.24	0.34	0.26	0.17	0.31	0.34	0.28	0.30	0.29	0.36	0.30	0.30	0.28	0.35	0.20	0.08	0.26
LOI	6.47	3.62	2.33	5.41	3.11	5.69	6.26	5.61	5.08	3.92	2.82	5.62	8.53	4.58	5.51	2.84	5.34	3.23	1.94	5.22
Total	100.03	99.89	100.02	99.94	100.00	99.54	99.93	99.97	99.85	100.01	99.95	99.96	99.75	99.77	100.03	100.01	99.88	99.97	99.98	99.77
Mg#*	0.48	0.45	0.38	0.47	0.35	0.47	0.58	0.54	0.44	0.35	0.51	0.44	0.43	0.49	0.53	0.52	0.49	0.58	0.48	0.51
Sc	32.8	37.9	26.5	27.6	31.0	49.7	38.5	29.6	31.1	28.0	26.8	28.9	19.7	27.4	29.6	22.1	31.9	12.6	11.2	35.0
V	214	205	121	237	218	411	329	304	246	286	283	239	209	282	309	285	346	163	157	263
Cr	112.0	113.0	105.0	108.0	131.0	130.0	156.0	117.0	107.0	77.3	87.8	121.0	237.0	181.0	123.0	129.0	152.0	115.0	97.0	140.0
Ni	54.5	62.0	45.9	45.8	64.1	72.2	66.8	50.8	50.5	45.9	53.5	54.7	30.1	45.1	50.7	44.7	53.4	28.9	28.6	72.2
Cu	26.7	39.3	16.1	38.2	8.99	35.5	96.1	67.1	20.5	9.64	58.9	66.8	6.08	5.08	66.3	10.4	5.63	59.8	56.6	62.5
Zn	168.0	125.0	89.8	162.0	112.0	198.0	113.0	207.0	113.0	90.6	133.0	129.0	71.5	122.0	202.0	124.0	154.0	58.4	57.6	125.0
Rb	2.52	87.90	72.70	4.00	118.00	11.30	111.00	3.22	6.30	20.80	7.15	11.00	118.00	109.00	3.18	96.60	113.00	70.80	112.40	73.70
Sr	124.0	58.0	67.6	113.0	77.6	106.0	316.0	153.0	112.0	91.4	557.0	94.2	75.5	162.0	160.0	171.0	171.0	365.0	413.0	155.0
Ba	44.6	708.0	672.0	61.9	921.0	85.7	132.0	39.2	99.5	175.0	78.7	97.8	966.0	526.0	40.0	703.0	554.0	87.0	241.0	303.0
U	0.656	0.880	0.676	0.557	1.120	0.969	0.498	0.475	0.662	0.593	0.583	0.562	2.140	0.974	0.466	1.790	1.220	0.448	2.290	0.587
Th	2.46	4.03	3.06	2.51	3.30	2.92	0.94	2.74	2.67	2.72	2.90	2.52	16.0	9.19	2.70	15.5	6.90	0.86	13.40	2.25
Y	26.2	28.3	29.2	26.5	31.4	30.5	19.7	27.3	26.6	25.1	26.4	26.0	39.9	44.3	27.2	36.7	52.7	29.2	30.7	24.6
Zr	126	184	145	130	175	142	94	140	136	142	140	119	470	189	138	363	250	89	307	133
Nb	12.3	18.6	14.5	12.9	17.5	14.9	10.2	13.8	13.6	14.0	14.5	12.6	40.3	22.6	13.9	37.3	28.7	10.0	10.3	14.1
Ga	18.3	20.5	20.1	18.0	24.5	23.1	18.5	22.3	18.5	18.6	18.6	18.9	24.9	16.3	21.6	21.4	19.8	19.3	19.1	18.1

Hf	3.16	4.85	3.86	3.28	4.42	3.76	2.48	3.51	3.55	3.56	3.93	3.33	13.20	5.28	3.62	9.73	6.72	2.41	8.95	3.62
Ta	0.88	1.36	1.06	0.90	1.22	1.02	0.76	0.96	1.19	0.98	1.21	0.92	3.03	1.74	0.98	3.24	1.85	0.76	1.04	1.03
La	18.6	39.3	27.1	20.3	30.6	25.0	9.4	22.7	23.4	23.4	23.9	21.6	57.0	28.7	23.2	93.0	37.0	9.8	23.1	23.6
Ce	38.2	73.7	57.6	42.0	61.8	49.9	21.9	45.8	45.3	47.5	48.8	42.6	111.0	56.0	47.3	168.0	72.0	22.2	49.4	48.9
Pr	5.17	8.56	7.16	5.38	8.00	6.59	3.21	5.94	5.93	6.11	6.47	5.65	13.6	7.92	6.22	21.3	9.97	3.33	6.26	6.28
Nd	22.3	34.2	29.6	22.3	33.1	27.5	14.7	24.6	24.7	25.4	26.9	23.8	51.4	32.8	25.8	78.5	40.7	15.2	24.2	27.7
Sm	4.39	6.54	5.97	4.56	6.69	5.59	3.56	4.97	4.90	4.95	5.45	4.75	9.20	6.98	5.21	12.20	8.53	3.63	4.96	5.63
Eu	1.44	2.44	1.93	1.57	2.07	1.87	1.30	1.71	1.59	1.63	1.80	1.61	2.18	3.45	1.80	2.63	4.11	1.39	1.47	1.94
Gd	4.89	7.29	6.60	5.13	7.59	6.05	4.35	5.63	5.33	5.40	6.04	5.19	8.50	8.47	5.67	9.71	10.00	4.32	5.14	6.31
Tb	0.731	1.060	1.020	0.756	1.103	0.916	0.650	0.855	0.816	0.826	0.914	0.781	1.360	1.400	0.872	1.440	1.560	0.667	0.918	0.928
Dy	4.23	5.91	5.84	4.43	6.36	5.23	3.75	4.87	4.75	4.72	5.24	4.50	7.79	8.28	5.07	8.01	9.25	3.78	5.90	5.26
Ho	0.851	1.14	1.21	0.876	1.28	1.04	0.743	0.959	0.954	0.936	1.03	0.896	1.59	1.64	1.02	1.61	1.85	0.752	1.29	0.980
Er	2.20	2.80	3.22	2.26	3.32	2.66	1.88	2.52	2.47	2.44	2.71	2.33	4.16	4.01	2.62	4.40	4.66	1.90	3.63	2.44
Tm	0.342	0.411	0.504	0.347	0.508	0.408	0.290	0.382	0.382	0.370	0.402	0.355	0.652	0.572	0.408	0.705	0.691	0.288	0.607	0.354
Yb	2.17	2.49	3.10	2.21	3.22	2.55	1.74	2.39	2.39	2.30	2.52	2.28	4.14	3.34	2.47	4.57	4.03	1.77	3.79	2.19
Lu	0.352	0.384	0.521	0.360	0.513	0.414	0.272	0.374	0.382	0.361	0.402	0.361	0.672	0.462	0.395	0.791	0.583	0.273	0.609	0.331
ΣREE	106	186	151	112	166	136	67.7	124	123	126	133	117	273	164	128	407	205	69.4	131	133
Gd/Yb	2.3	2.9	2.1	2.3	2.4	2.4	2.5	2.4	2.2	2.3	2.4	2.3	2.1	2.5	2.3	2.1	2.5	2.4	1.4	2.9
La/Nb	1.5	2.1	1.9	1.6	1.7	1.7	0.9	1.6	1.7	1.7	1.7	1.7	1.4	1.3	1.7	2.5	1.3	1.0	2.2	1.7
Th/Nb	0.20	0.22	0.21	0.20	0.19	0.20	0.09	0.20	0.20	0.19	0.20	0.20	0.40	0.41	0.19	0.42	0.24	0.09	1.29	0.16
Zr/Nb	10	10	10	10	10	9.5	9.2	10	10	10	9.6	9.5	12	8.4	10	9.7	8.7	9.0	30	9.4
Ti/Zr	93	99	94	95	91	100	136	93	96	90	94	100	23	71	92	33	71	131	18	107
Ti/Y	446	649	468	466	510	465	649	478	491	510	498	456	275	304	467	324	339	403	183	577
La/Yb	8.6	15.8	8.7	9.2	9.5	9.8	5.4	9.5	9.8	10.1	9.5	9.4	13.8	8.6	9.4	20.4	9.2	5.6	6.1	10.8
Zr/Y	4.8	6.5	5.0	4.9	5.6	4.6	4.8	5.1	5.1	5.7	5.3	4.6	11.8	4.3	5.1	9.9	4.7	3.1	10.0	5.4
Hf/Ta	3.6	3.6	3.7	3.6	3.6	3.7	3.2	3.6	3.0	3.6	3.3	3.6	4.4	3.0	3.7	3.0	3.6	3.2	8.6	3.5
Ta/Yb	0.40	0.55	0.34	0.41	0.38	0.40	0.44	0.40	0.50	0.43	0.48	0.40	0.73	0.52	0.40	0.71	0.46	0.43	0.27	0.47
Th/Yb	1.1	1.6	1.0	1.1	1.0	1.1	0.5	1.1	1.1	1.2	1.2	1.1	3.9	2.8	1.1	3.4	1.7	0.5	3.5	1.0
Eu/Eu*†	0.95	1.08	0.94	1.00	0.89	0.98	1.01	0.99	0.95	0.96	0.96	0.99	0.75	1.37	1.01	0.74	1.36	1.07	0.89	1.00
Ce/Ce*‡	0.91	0.94	0.97	0.94	0.93	0.91	0.94	0.93	0.90	0.93	0.92	0.90	0.93	0.87	0.92	0.88	0.88	0.91	0.96	0.94
Nb/Nb*§	0.62	0.50	0.54	0.61	0.59	0.59	1.16	0.59	0.58	0.60	0.59	0.58	0.45	0.47	0.59	0.33	0.61	1.16	0.20	0.65

*Mg# (Mg number) = (MgO/40.4)/[(MgO/40.4) + 0.85*$Fe_2O_3^T$*0.70/(0.78*77.8)].

†Eu/Eu* = (Eu/0.087)/(Sm*Gd/0.306/0.231)$^{\frac{1}{2}}$.

‡Ce/Ce* = (Ce/0.957)/(La*Pr/0.367/0.137)$^{\frac{1}{2}}$.

§Nb/Nb* = 0.3384*Nb/(Th*La)$^{\frac{1}{2}}$.

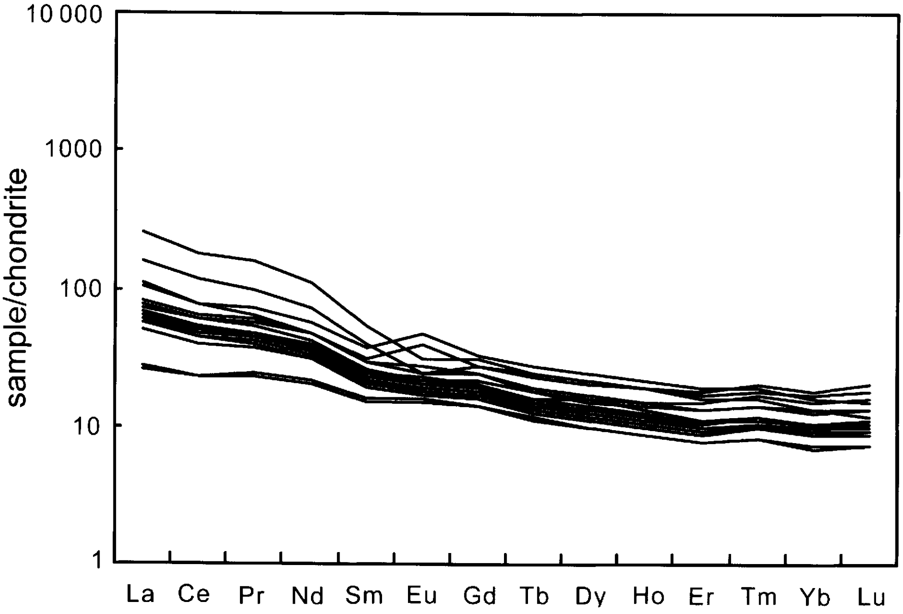

Fig. 4. Chondrite-normalized rare-earth element patterns for the Akaz metavolcanic rocks (chondrite values from Taylor & McLennan 1985).

diagram (Pearce 1983) (most rocks plot in the active continental margin field; Fig. 7b).

Although the Akaz metavolcanics exhibit some characteristics of within-plate basalts, they cannot have been derived from ocean floor, oceanic plateau or mature back-arc basin basalts,

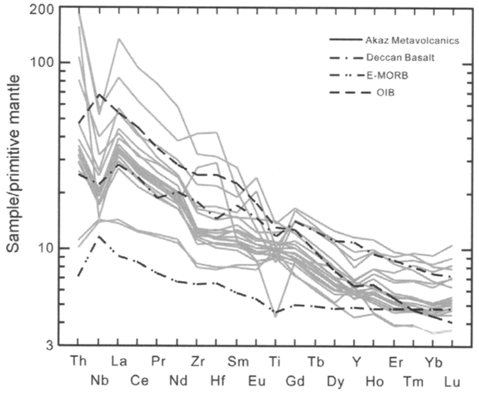

Fig. 5. Primitive-mantle-normalized spider diagram for the Akaz metavolcanic rocks (primitive mantle, E-MORB and OIB values from Sun & McDonough 1989; Deccan basalt data from Wilson 1989).

because they are more enriched than these lavas and have significant negative Nb anomalies (Floyd 1989; Wilson 1989; Saunders & Tarney 1991) (Figs 4 and 5). Ocean island basalts are generally considered to originate from plume-related sources (Wilson 1989; Floyd 1991), whereas seamount basalts have complicated geochemical characteristics that strongly depend on the tectonic settings. Seamounts in within-oceanic plate settings have been explained as the products of hot-spots (e.g. Clague & Dalrymple 1987); however, some seamounts occur in suprasubduction zone environments, and their lavas can be imprinted with a strong subduction-related signature (e.g. Kamenetsky *et al.* 1997). The within-plate characteristics of the Akaz metavolcanic rocks and their association with limestone have led some researchers to suggest that these rocks formed as part of a seamount (Xiao *et al.* 2002). Although these metavolcanic rocks have trace-element concentrations and some element ratios close to those of E-MORB or OIB, their Nb/La ratios (0.4–1.1) are significantly lower than modern OIB or E-MORB (*c.* 1.3) (Sun & McDonough 1989).

The relatively LREE- and LILE-enriched compositions and negative Nb anomalies are characteristics of subduction-related basalts or

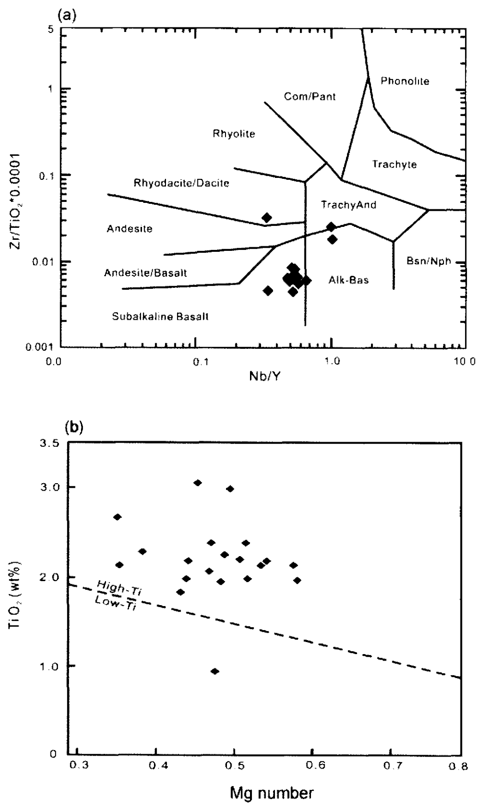

Fig. 6. Classification diagrams for the Akaz metavolcanic rocks. (**a**) Nomenclature of the Akaz metavolcanic rocks (after Winchester & Floyd 1977); (**b**) Correlation diagram of Mg number and TiO_2 for the Akaz metavolcanic rocks (after Lightfoot 1993).

contaminated continental flood/rift basalts. Partial melting induced by dehydration of a subducting slab in the mantle (Pearce & Parkinson 1993; Thirlwall *et al.* 1994; Tatsumi & Eggins 1995), and contamination of continental crust (Dupuy & Dostal 1984; Cox & Hawkesworth 1985; Arndt *et al.* 1993; Cadman *et al.* 1995) may produce basalts with Nb–Ta depletions. The subduction-related basalts generated in intra-oceanic island arcs and active continental margins can be effectively distinguished by their incompatible element ratios. When compared with typical intra-oceanic arc basalts (Zr/Y <3; Ta/Yb <0.1 and $25 < Zr/Nb < 70$) (Condie 1989; McCulloch & Gamble 1991), the Akaz rocks have high Zr/Y (3–12), Ta/Yb (0.3–0.7) and low Zr/Nb (mostly <12) ratios, strongly supporting a continental affinity (Table 1, Fig. 7b). This precludes intra-oceanic arc basalts as the protolith of these rocks, and the transitional geochemical characteristics between within-plate basalts and arc-related basalts indicate that the most likely protolith is either subduction-related basalts in an active continental margin, or continental flood/rift basalts contaminated with crustal materials. Continental flood basalts usually have steeply sloping heavy rare-earth element patterns that are rarely seen in arc tholeiites (Arndt, pers. comm.). Data for the Akaz metavolcanic rocks, continental flood basalts and island arc tholeiites are compared in a Gd/Yb v. Gd diagram (Fig. 8). Except for one sample

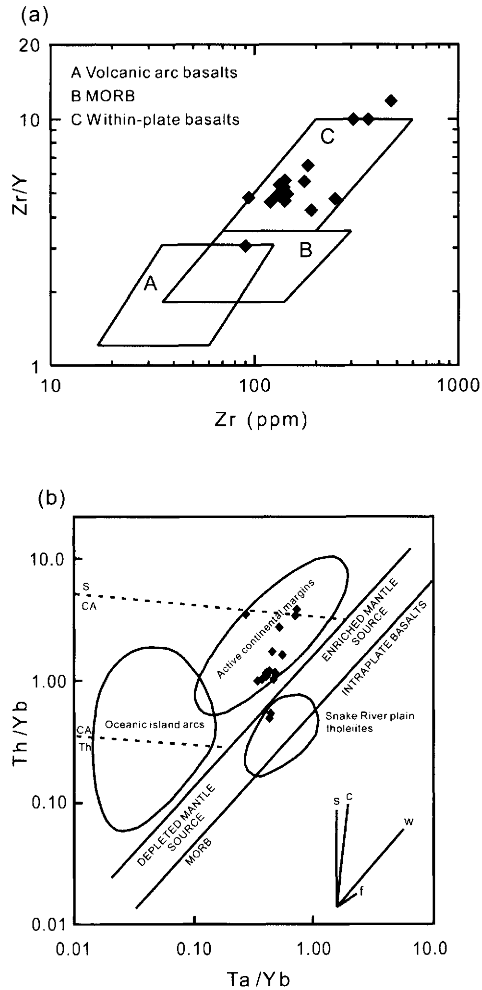

Fig. 7. Immobile-element-based tectonic discrimination diagrams for the Akaz metavolcanic rocks: (**a**) Zr v. Zr/Y diagram (after Pearce 1983); (**b**) Th/Yb versus Ta/Yb diagram (after Pearce 1983). Vectors shown indicate the influence of a subduction component (s), within-plate enrichment (w), crustal contamination (c) and fractional crystallization (f).

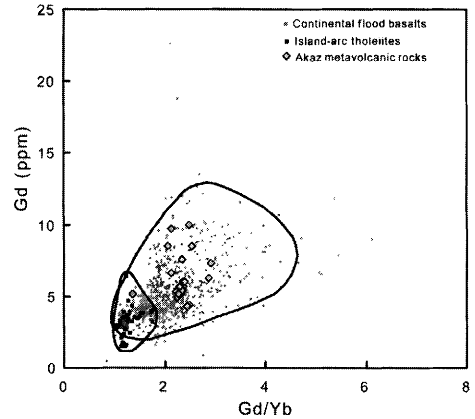

Fig. 8. Discrimination diagram of Gd/Yb v. Gd for the Akaz metavolcanic rocks. CFB, continental flood basalts; IAT, island-arc tholeiites (fields are drawn based on data from the GEOROC database, Max-Planck-Institut für Chemie).

(GS-19, $SiO_2 = 64.7$ wt%), most of the Akaz metavolcanic rocks plot in the CFB field (Fig. 8). The existence of E-MORB-type samples and the transitional nature of the other samples suggest that the Akaz metavolcanic rocks were derived from contaminated continental rift basalts. Some tholeiitic samples in Fig. 6a contain relatively high K_2O contents (Table 1), which also suggests assimilation of crustal materials. The most Nb-depleted sample GS-19 ($Nb/Nb^{\#} = 0.2$) has the highest SiO_2 (64.7 wt%) and lowest TiO_2 (0.94 wt%) contents and displays a Zr–Hf peak (Zr/Sm = 62) in its trace-element pattern (Table 1; Fig. 5), reflecting the most intensive crustal contamination. Samples GS-7 and GS-18 exhibit slightly positive Nb-anomalies, and are characterized by the lowest LILE and LREE contents (Fig. 5), and may represent the uncontaminated primary magma.

Further constraints on the tectonic setting of the Akaz metavolcanic rocks come from field evidence. The Sailajaz Tagh Group has a total thickness of about 3500 m, only about one-tenth of which is occupied by the metavolcanic rocks (XGIT-II 1985). Typical continental flood basalts, e.g. Deccan and Siberian traps (Mahoney 1988; Zolotukhin & Al'mukhamedov 1988) are much thicker than this, suggesting a continental rift environment for the Akaz lavas.

Implications for the separation of Tarim from Gondwana

No consensus has been reached on the tectonic evolution of the Kunlun Mountains. A number of authors have accepted the arc–continental collisional model to explain the accretion of the Kunlun Mountains along the southern margin of the Tarim craton (Yao & Hsü 1994; Hsü *et al.* 1995; Sengör & Natal'in 1996; Li *et al.* 1999; Xiao *et al.* 2002), whereas others consider the South Kunlun Block as a microcontinental block, rifted from the Tarim craton (Pan *et al.* 1994; Ding *et al.* 1996; Jiang *et al.* 2000). Granitoids of the South Kunlun Block, regardless of their ages and tectonic setting, all have young T_{DM} ages (1.0 to 1.5 Ga) (Yuan *et al.* 2003). These young T_{DM} ages are consistent with those of the metamorphic complex in the South Kunlun Block (Zhou 1998), but significantly different from those of the North Kunlun Block (2.8 Ga) (Arnaud & Vidal 1990). These features suggest that the South Kunlun Block does not have an Archean basement and is probably an ancient accretionary prism (Yuan *et al.* 2003).

The available palaeomagnetic and stratigraphic data show that the Tarim Craton was originally part of Gondwana (e.g. Li *et al.* 1991; Li *et al.* 1996; Metcalfe 1996; Zhao *et al.* 1996; Li, 1998; Stampfli & Borel 2002). However, there is little agreement as to when the Tarim Craton rifted from Gondwana. Some workers suggest that rifting took place in the Neoproterozoic as the Rodinia supercontinent dispersed (Li *et al.* 1996; Li 1998), whereas others propose a Devonian or later rifting event (Metcalfe 1996; Zhao *et al.* 1996; Li 1998; Stampfli & Borel 2002). This study indicates that the Akaz metavolcanic rocks formed in a continental rift environment along the south margin of the Tarim Craton. Although precise radiometric data are not available, the Akaz metavolcanic rocks are certainly Sinian to Early Cambrian based on palaeontological and stratigraphic studies of the associated sedimentary rocks (Pan *et al.* 1994; Xiao *et al.* 2002). Coeval continental rift volcanism has also been recently recognized in the East Kunlun (Pan *et al.* 1996) and North Qilian (Xia *et al.* 1996; Mao *et al.* 1998; Zuo *et al.* 1999) orogenic belts. These findings support a pre-Devonian rifting age.

Conclusions

The Akaz metavolcanic rocks were metamorphosed from a high-Ti tholeiitic protolith, with characteristics transitional between within-plate and subduction-related basalts. LREE-enriched patterns and negative Nb anomalies in most samples preclude oceanic environments (ocean floor, within-plate seamount, oceanic island or plateau basalts) for the protolith. The high Zr/Y, Ta/Yb, Gd/Yb and low Zr/Nb ratios strongly support a continental affinity and make the Akaz metavolcanic rocks distinct from island–arc tholeiites. The existence of a few E-MORB-like samples, undepleted in Nb, indicate that the Akaz metavolcanic rocks were originally continental rift basalts contaminated by crustal materials. The Akaz metavolcanic rocks, together with other continental rift volcanic rocks in the East Kunlun and North Qilian orogenic belts, provide evidence for rifting of the Tarim Craton from Gondwana in the Sinian or Early Cambrian.

We are grateful to Li Jiliang, Zhang Yuquan, Pan Yusheng, Xu Ronghua, Xiao Wenjiao and Hou Quanlin for their fruitful discussions about the tectonic evolution of the Kunlun Mountains. Special thanks are given to Brian Windley for his enlightening suggestions. N. T. Arndt and P. Black are greatly thanked for their constructive and encouraging reviews. We gratefully thank P. Robinson for his kind help in the revision of the manuscript. This research was supported by Chinese Project 973 (G1998040800), NSF of China (project 40003005), and an Outstanding Researcher Award from the University of Hong Kong.

References

ARNAUD, N. & VIDAL, PH. 1990. Geochronology and geochemistry of the magmatic rocks from the Kunlun–Karakorum geotraverse. *Colloque Kunlun–Karakorum, IGP' Paris*, 52.

ARNDT, N. T., CZAMANSKE, G. K., WOODEN, J. L. & FEDORENKO, V. A. 1993. Mantle and crustal contributions to continental flood volcanism. *Tectonophysics*, **223**, 39–52.

CADMAN, A. C., TARNEY, J. & BARAGAR, W. R. A. 1995. Nature of mantle source contributions and the role of contamination and *in situ* crystallization in the petrogenesis of Proterozoic mafic dykes and flood basalts, Labrador. *Contributions to Mineralogy and Petrology*, **122**, 213–229.

CHANG, C. F., CHEN, N. S. *et al.* 1986. Preliminary conclusions of the Royal Society and Academia Sinica 1985 geotraverse of Tibet. *Nature*, **323**, 501–507.

CLAGUE, D. A. & DALRYMPLE G. B., 1987. The Hawaiian-Emperor volcanic chain, Part I, Geological evolution. *In:* DECKER, R. W., WRIGHT, T. & STAUFFER, P. H. (eds). Volcanism in Hawaii: *US Geological Survey Professional Paper*, **1350**, 5–54.

CONDIE, K. C. 1989. Geochemical changes in basalts and andesites across the Archean–Proterozoic boundary: identification and significance. *Lithos*, **23**, 1–18.

COX, K. G. & HAWKESWORTH, C. J. 1985. Geochemical stratigraphy of the Deccan Traps, at Mahabaleshwar, Western Ghats, India, with implications for open system magmatic processes. *Journal of Petrology*, **26**, 355–377.

DENG, W. 1989. A preliminary study on the basic–ultrabasic rocks of the Karakorum–western Kunlun Mts. *Journal of Natural Resources*, **4**, 204–211 (in Chinese with English abstract).

DEWEY, J. F., SHACKLETON, R. M., CHANG, C. F. & SUN, Y. Y. 1988. The tectonic evolution of the Tibetan Plateau. *Philosophical Transactions of the Royal Society of London*, **327**, 379–413.

DING, D., SHAN, X. & ZHANG, Y. 1996. The basin protype and sedimentary–tectonic subdivision of South Tarim and West Kunlun Orogens. *In:* DING, D., WANG, D., LIU, W. & SUN, S. (eds) *The Western Kunlun Orogenic Belt and Basin.* Geological Publishing House, Beijing, China, 9–35 (in Chinese, with English summary).

DUPUY, C. & DOSTAL, J. 1984. Trace element geochemistry of some continental tholeiites. *Earth and Planetary Sciences Letters*, **67**, 61–69.

FLOWER, M. 1991. Magmatic processes in oceanic ridge and intraplate settings. *In:* FLOYD, P. A. (ed.) *Oceanic Basalts*. Blackie, Glasgow & London and Van Nostrand Reinhold, New York, 116–147.

FLOYD, P. 1989. Geochemical features of intraplate oceanic plateau basalts. *In:* SAUNDERS, A. D. & NORRY, M. J. (eds) *Magmatism in the Ocean Basin*. Geological Society, London, Special Publications, **42**, 215–230.

FLOYD, P. 1991. Oceanic islands and seamounts. *In:* FLOYD, P. A. (ed.) *Oceanic Basalts*. Blackie, Glasgow and London, and Van Norstrand Reinhold, New York, 174–218.

HSÜ, K. J., PAN, G. *et al.* 1995. Tectonic evolution of the Tibetan Plateau: a working hypothesis based on the archipelago model of orogenesis. *International Geology Review*, **37**, 473–508.

JIANG, C. F., WANG, Z. Q. & LI, J. Y. 2000. *Opening–closure tectonics of Chinese central orogenic belt.* Geological Publishing House, Beijing, 1–153 (in Chinese with English abstract).

KAMENETSKY, V. S., CRAWFORD, A. J., EGGINS, S. & MÜHE, R. 1997. Phenocryst and melt inclusion chemistry of near axis seamounts, Valu Fa Ridge, Lao Basin: insight into mantle wedge melting and the addition of subduction components. *Earth and Planetary Science Letters*, **151**, 205–223.

LI, J., SUN, S., HAO, J., CHEN, H., HOU, Q. & XIAO, W. 1999. On the classification of collision orogenic belts. *Scientia Geologica Sinica*, **34**, 129–138 (in Chinese with English abstract).

LI, Y. P., LI, Y. A., SHARPS, R., MCWILLIAMS, M., & GAO, Z. J. 1991. Sinian palaeomagnetic results from the Tarim block, western China. *Precambrian Research*, **49**, 61–67.

LI, Z. X. 1998. Tectonic history of the major East Asian lithospheric blocks since the Mid-Proterozoic–a synthesis. *In:* FLOWER, M. F. J., CHUNG, S. L., LO, C. H. & LEE, T. Y. (eds) *Mantle Dynamics and Plate Interactions in East Asia*. American Geophysical Union, Geodynamics Series, **27**, 221–243.

LI, Z. X., ZHANG, L. & POWELL, C. MCA. 1996. Positions of the East Asian cratons in the Neoproterozoic supercontinent Rodinia. *Australian Journal of Earth Sciences* **43**, 593–604.

LIGHTFOOT, P. C. 1993. The interpretation of geoanalytical data. *In:* RIDDLE, C. (ed.) *Analysis of*

Geological Materials. Marcel Dekker, New York, 377–455.

McCulloch, E. M. & Gamble, J. A. 1991. Geochemical and geodynamic constraints on subduction magmatism. *Earth and Planetary Science Letters*, **102**, 358–374.

Mahoney, J. J. 1988. Deccan traps. *In:* Macdougall, J. D. (ed.) *Continental Flood Basalts*. Kluwer Academic Publishers, Dordrecht, Netherlands, 151–194.

Mao, J., Zhang, Z., Yang, J., Song, B., Wu, M. & Zuo, G. 1998. Single-zircon dating of Precambrian strata in the west sector of the northern Qilian Mountains and its geological significance. *Chinese Science Bulletin*, **43**, 1289–1294.

Matte, Ph., Tapponnier, P., Arnaud, N., Bourjot, L., Avouac, Vidal, Ph., Liu, Q., Pan, Y. S. & Wang, Y. 1996. Tectonics of Western Tibet, between the Tarim and the Indus. *Earth and Planetary Science Letters*, **142**, 311–330.

Mattern, F. & Schneider, W. 2000. Suturing of the Proto- and Paleo-Tethys oceans in the western Kunlun (Xinjiang, China). *Journal of Asian Earth Sciences*, **18**, 637–650.

Mattern, F., Schneider, W., Li, Y. & Li, X. 1996. A traverse through the western Kunlun (Xinjiang, China): tentative geodynamic implications for the Paleozoic and Mesozoic. *Geologische Rundschau*, **85**, 705–722.

Metcalfe, I. 1996. Gondwanaland dispersion, Asian accretion and evolution of eastern Tethys. *Australia Journal of Earth Sciences*, **43**, 605–623.

Molnar, P., Burchfiel, B. C., Zhao, Z., Liang, K., Wang, S. & Huang, M. 1987. Geological evolution of northern Tibet: results of an expedition to Ulugh Muztagh. *Science*, **235**, 299–304.

Pan, Y. S., Wang, Y., Matte, Ph. & Tapponnier, P. 1994. Tectonic evolution along the geotraverse from Yecheng to Shiquanhe. *Acta Geologica Sinica*, **68**, 295–307 (in Chinese with English abstract).

Pan, Y., Zhou, W. *et al.* 1996. Early Paleozoic geological characteristics and tectonic evolution. *Science in China (Series D)*, **26**, 302–307 (in Chinese).

Pearce, J. A. 1983. Role of the sub-continental lithosphere in magma genesis at active continental margins. *In:* Hawkesworth, C. J. & Norry, M. J. (eds) *Continental Basalts and Mantle Xenoliths*. Shiva, Nantwich, 230–249.

Pearce, J. A. & Cann, J. R. 1973. Tectonic setting of basic volcanic rocks determined using trace element analyses. *Earth and Planetary Science Letters*, **19**, 290–300.

Pearce, J. A. & Parkinson, I. J. 1993. Trace element models for mantle melting: application to volcanic arc petrogenesis. *In:* Prichard, H. M., Alabaster, T., Harris, N. B. W. & Neary, C. R. (eds) *Magmatism Processes and Plate Tectonics*. Geological Society, London, Special Publications, **76**, 373–403.

Saunders, A. & Tarney, J. 1991. Back-arc basins. *In:* Floyd, P. A. (ed.) *Oceanic Basalts*. Blackie, Glasgow and London; Van Nostrand Reinhold, New York, 219–263.

Sengör, A. M. C. & Natal'in, B. A. 1996. Paleotectonics of Asia: fragments of a synthesis. *In:* Yin, A. & Harrison, T. M. (eds) *The Tectonic Evolution of Asia*. Cambridge University Press, 486–640.

Stampfli, G. M. & Borel, G. D. 2002. A plate tectonic model for the Paleozoic and Mesozoic constrained by dynamic plate boundaries and restored synthetic oceanic isochrones. *Earth and Planetary Science Letters*, **196**, 17–33.

Sun, S-s. & McDonough, W. F. 1989. Chemical and isotopic systematics of oceanic basalts: implications for mantle composition and processes. *In:* Saunders, A. D. & Norry, M. J. (eds) *Magmatism in the Ocean Basins*. Geological Society, London, Special Publications, **42**, 313–346.

Tatsumi, Y. & Eggins, S. 1995. *Subduction Zone Magmatism*. Blackwell Science, Cambridge, MA.

Taylor, S. R. & McLennan, S. M. 1985. *The Continental Crust: its Composition and Evolution: an Examination of the Geochemical Record Preserved in Sedimentary Rocks*. Blackwell Scientific Publications, Oxford.

Thirlwall, M. F., Smith, T. E., Graham, A. M., Theodorou, N., Hollings, P., Davidson, J. P. & Arculus, R. J. 1994. High field strength element anomalies in arc lavas: source or process? *Journal of Petrology*, **35**, 819–838.

Wen, S., Sun, D., Yin, J., Chen, T. & Luo, H. 2000. Stratigraphy and paleontology. *In:* Pan, Y. (ed.) *Geological Evolution of the Karakorum and Kunlun Mountains*. Science Press, Beijing, 6–92 (in Chinese).

Williams, H., Turner, F. J. & Gilbert, C. M. 1989. *Petrography – An Introduction to the Study of Rocks in Thin Sections, 2nd edn*, W. H. Freeman, San Francisco.

Wilson, M. 1989. *Igneous Petrogenesis*. Unwin Hyman, London.

Winchester, J. A. & Floyd, P. A. 1977. Geochemical discrimination of different magma series and their differentiation products using immobile elements. *Chemical Geology*, **20**, 325–343.

XGIT-II 1985. *Stratigraphy, 1/500,000 geological map and explanation of Southwestern Xinjiang, China*. Geological Publishing House, Beijing.

Xia, L., Xia, Z., Zhao, J., Xu, X., Yang, H. & Zhao, D. 1999. Determination of properties of Proterozoic continental flood basalts of western part from North Qilian Mountains. *Science in China (Series D)*, **42**, 506–514.

Xia, Z., Xia, L. & Xu, X. 1996. The Late Proterozoic–Cambrian active continental rift volcanism in northern Qilian mountains. *Acta Geoscientia Sinica*, **17**, 282–291 (in Chinese with English abstract).

Xiao, W. J., Windley, B. F., Hao, J. & Li, J. L. 2002. Arc-ophiolite obduction in the Western Kunlun Range (China): implications for the Paleozoic evolution of central Asia. *Journal of the Geological Society of London*, **159**, 517–528.

Xu, R., Zhang, *et al.* 1994. A discovery of an early Palaeozoic tectono-magmatic belt in the Northern part of west Kunlun Shan. *Scientia Geologica*

Sinica, **29**, 313–328 (in Chinese with English abstract).

YANG, J. S., ROBINSON, R. T., JIANG, C. F. & XU, Z. Q. 1996. Ophiolites of the Kunlun Mountains, China and their tectonic implications. *Tectonophysics*, **258**, 215–231.

YAO, Y. & HSÜ, K. J. 1994. Origin of the Kunlun Mountains by arc–arc and arc–continent collisions. *The Island Arc*, **3**, 75–89.

YIN, A. & HARRISON, T. M. 2000. Geologic evolution of the Himalayan–Tibetan Orogen, *Annual Review of Earth and Planetary Sciences*, **28**, 211–280.

YUAN, C., SUN, M., ZHOU, M. F., ZHOU, H., XIAO, W. J. & LI, J. I. 2002. Tectonic evolution of the West Kunlun: geochronologic and geochemical constraints from Kudi Granitoids. *International Geology Review*, **44**, 653–669.

YUAN, C., SUN, M., ZHOU, M. F., ZHOU, H., XIAO, W. J. & LI, J. L. 2003. Absence of Archean basement in the South Kunlun Block: Nd–Sr–O isotopic evidence from granitoids. *The Island Arc*, **12**, 13–21.

ZHAO, X., COE, R. S., GILDER, S. A. & FROST, G. M. 1996. Paleomagnetic constraints on the palaeogeography of China: implications for Gondwanaland. *Australian Journal of Earth Sciences*, **43**, 643–672.

ZHOU, H. 1998. *The main ductile shear zone and the lithosphere effective elastic thickness of west Kunlun orogenic belt*. PhD thesis, Institute of Geology, Chinese Academy of Sciences, Beijing, China (in Chinese with English abstract).

ZOLOTUKHIN, V. V. & AL'MUKHAMEDOV, A. I. 1988. Traps of the Siberian Platform. *In:* MACDOUGALL, J. D. (ed.) *Continental Flood Basalts*, 273–310, Kluwer Academic Publishers, Dordrecht, Netherlands.

ZUO, G., WU, M., MAO, J. & ZHANG, Z. 1999. Structural evolution of Early Paleozoic tectonic belt in the west section of northern Qiliang area. *Acta Geologica Gansu*, **8**, 6–13 (in Chinese with English abstract).